Electronic Supplementary Material (ESI) for Organic Chemistry Frontiers.

meso-to-*meso* Pt^{II}-Bridged Porphyrin Dimers: one-electron oxidation induced reductive elimination

Norihito Fukui, Hua-Wei- Jiang, and Atsuhiro Osuka*

Department of Chemistry, Graduate School of Science, Kyoto University, Sakyo-ku, Kyoto 606-8502, Japan.

Contents

1. Instrumentation and Materials

^{1}H NMR (600 MHz), ^{13}C NMR (151 MHz), and ^{31}P NMR (243 MHz) spectra were taken on a JEOL ECA-600 spectrometer. Chemical shifts were reported as delta scale in ppm relative to $CHCl_3$ (δ = 7.26) for ^{1}H NMR, to $CDCl_3$ (δ = 77.16) for ^{13}C NMR, and to H_3PO_4 (δ = 0.00) for ^{31}P NMR. UV/Vis absorption spectra were recorded on a Shimadzu UV-3600 spectrometer. High-resolution ESI-TOF mass spectra were taken on a Bruker micrOTOF spectrometer. Redox potentials were measured by cyclic voltammetry method on an ALS model 660 electrochemical analyzer. X-Ray data were taken at −180 °C with a Rigaku XtaLAB P200 diffractometer by using graphite monochromated Cu-K$_\alpha$ radiation (λ = 1.54187 Å). The structures were solved by using direct methods (SIR-97,[S1] SHELX-97,[S2] or SHELXT[S3] programs). Structure refinements were carried out by using SHELXL-2014/7 program.[S4] CCDC numbers 1529198 (**5**) and 1529199 (**7**) contain supplementary crystallographic data for this paper. These data can be obtained free of charge from the Cambridge Crystallographic Data Centre via www.ccdc.cam.ac.uk/data_request/cif. Preparative separations were performed by silica gel column chromatography (Wako gel C-200, C-300, and C-400). The anodic oxidation was carried out using an H-type divided cell equipped with an anode made of a Pt wire and a cathode made of a Pt wire as shown in the following picture. The constant current was generated by a YAZAWA CS-12Z DC power supply. CH_2Cl_2 for anodic oxidation was purified by passing through an alumina column, dehydrated by a molecular sieve 4A, and degassed by N_2 bubbling. THF was purified by passing through a neutral alumina column under N_2. Toluene was distilled from CaH_2. Unless otherwise noted, materials obtained from commercial suppliers were used without further purification.

2. Experimental Procedures and Compound Data

Synthesis of 5: A flask containing *meso*-borylporphyrin **8** (106 mg, 100 μmol), Pt(cod)Cl_2 (18.7 mg, 50 μmol), and CsF (304 mg, 2.0 mmol) was purged with nitrogen, and then charged with THF (5.0 mL). The mixture was stirred at 60 °C for 2 days. The residue was diluted with CH_2Cl_2, and passed through a small plug of silica-gel with copious washings (CH_2Cl_2). After removal of the solvent *in vacuo*, the residue was separated by silica gel chromatography eluting with CH_2Cl_2/*n*-hexane (1:4). Recrystallization of the separated solids from CH_2Cl_2/MeOH gave **5** (36.5 mg, 16.9 μmol, 34%).

5: ^{1}H NMR (600 MHz, $CDCl_3$, 25 °C): δ = 9.97 (d, J = 4.6 Hz, 4H, β), 8.66 (d, J = 4.6 Hz, 4H, β), 8.41 (d, J = 4.6 Hz, 4H, β), 8.34 (d, J = 4.6 Hz, 4H, β), 7.62 (t, J = 1.8 Hz, 4H, Ar-*p*), 7.47 (t, J = 1.8 Hz, 2H, Ar-*p*), 6.65 (br-s, 4H, cod), 4.41 (d, J = 9.7 Hz, 4H, cod), 2.95 (d, J = 9.7 Hz, 4H, cod), and 1.80-1.00 (br, 108H, *tert*-butyl) (The signals for some protons of the 3,5-di-*tert*-butylphenyl groups are too broad to analyze because of rotation of the *meso*-aryl groups.); ^{1}H NMR (600 MHz, $CDCl_3$, –60 °C): δ = 9.96 (d, J = 4.1 Hz, 4H, β), 8.70 (d, J = 4.1 Hz, 4H, β), 8.46 (d, J = 4.1 Hz, 4H, β), 8.36 (d, J = 4.1 Hz, 4H, β), 8.29 (s, 4H, Ar), 8.16 (s, 2H, Ar), 7.54 (s, 4H, Ar), 7.40 (s, 2H, Ar), 6.86 (s, 4H, Ar), 6.74 (br-s, 4H, cod), 6.61 (s, 2H, Ar), 3.51 (br-s, 4H, cod), 3.12 (br-s, 4H, cod), 1.58 (br-s, 36H, *tert*-butyl), 1.38 (br-s, 18H, *tert*-butyl), 1.20 (br-s, 36H, *tert*-butyl), and 1.02 (br-s, 18H, *tert*-butyl), ^{13}C NMR (151 MHz, $CDCl_3$, 50 °C): δ = 148.73, 148.67, 145.09, 142.08, 141.04, 140.65, 140.43, 140.30, 137.11, 135.72, 131.51, 131.31, 130.93, 128.55, 128.50, 120.71, 120.53, 117.76, 117.38, 109.45, 35.09, 34.91, 31.92, 31.73, and 30.75 ppm; ESI-TOF-MS: m/z = 2165.0670. Calcd for $C_{132}H_{154}N_8{}^{58}Ni^{60}Ni^{195}Pt$: 2165.0739 $[M+H]^+$; UV/Vis (CH_2Cl_2): λ_{max} (ε [$M^{-1}cm^{-1}$]) = 413 (3.28×10^5), 440 (9.99×10^4), 540 (2.87×10^4), and 580 (9.16×10^3) nm.

Synthesis of 6: A flask containing **5** (10.8 mg, 5.0 μmol) and 1,3-bis(diphenylphosphino)propane (DPPP, 10.3 mg, 25 μmol) was purged with nitrogen, and then charged with toluene (1.0 mL). The mixture was stirred at 110 °C for 4 h. After addition of $CHCl_3$ and *n*-hexane, the residue was separated by silica gel chromatography eluting with CH_2Cl_2/*n*-hexane (1:3). Recrystallization of the separated solids from CH_2Cl_2/MeOH gave **6** (7.9 mg, 3.2 μmol, 64%).

6: ^{1}H NMR (600 MHz, $CDCl_3$, 25 °C): δ = 10.27 (d, J = 5.0 Hz, 4H, β), 8.45 (d, J = 5.0 Hz, 4H, β), 8.43-8.40 (m, 8H, β), 7.90-7.40 (br, 12H, Ar-*o*), 7.60 (t, J = 1.9 Hz, 4H, Ar-*p*), 7.52 (t, J = 1.9 Hz, 2H, Ar-*p*), 6.94 (t, J = 7.7 Hz, 8H, dppp), 6.30-6.20 (m, 12H, dppp), 3.06 (br-s, 4H, dppp), 2.96 (br-s, 2H, dppp), 1.43 (br-s, 72H, *tert*-butyl), and 1.32 (br-s, 36H, *tert*-butyl); ^{31}P NMR (243 MHz, $CDCl_3$, 25 °C): δ = –7.15 (d, J_{PtP} = 1789 Hz) ppm; ESI-TOF-MS: m/z = 2465.1135. Calcd for $C_{151}H_{168}N_8{}^{58}Ni_2P_2{}^{194}Pt$: 2465.1196 $[M]^-$; UV/Vis (CH_2Cl_2): λ_{max} (ε [$M^{-1}cm^{-1}$]) = 419 (2.77×10^5), 445 (1.34×10^5), 544 (2.80×10^4), and 580 (9.99×10^3) nm.

Synthesis of 7: A flask containing **5** (10.8 mg, 5.0 μmol) and PPh_3 (13.1 mg, 50 μmol) was purged with nitrogen, and then charged with toluene (1.0 mL). The mixture was stirred at 120 °C for 3 h. The residue was diluted with CH_2Cl_2, and passed through a small plug of silica-gel with copious washings (CH_2Cl_2). After removal of the solvent *in vacuo*, the residue was separated by silica gel chromatography eluting with CH_2Cl_2/*n*-hexane (1:6).

Recrystallization of the separated solids from CH_2Cl_2/MeOH gave **7** (4.2 mg, 1.6 μmol, 33%).

7: ^{1}H NMR (600 MHz, $CDCl_3$, 25 °C): δ = 9.80 (d, J = 4.6 Hz, 4H, β), 8.65 (br-s, 8H, β), 8.36 (d, J = 4.6 Hz, 4H, β), 7.89 (d, J = 1.4 Hz, 4H, Ar-*o*), 7.87 (d, J = 1.9 Hz, 8H, Ar-*o*), 7.71 (t, J = 1.9 Hz, 4H, Ar-*p*), 6.68 (d, J = 1.4 Hz, 2H, Ar-*p*), 6.60-6.55 (m, 12H, PPh_3), 6.13 (t, J = 7.4 Hz, 6H, PPh_3), 6.00 (t, J = 7.4 Hz, 12H, PPh_3), 1.55 (s, 72H, *tert*-butyl), and 1.48 (s, 36H, *tert*-butyl); ^{31}P NMR (243 MHz, $CDCl_3$, 25 °C): δ = 12.57 (d, J_{PtP} = 2986 Hz) ppm; ESI-TOF-MS: m/z = 2577.1524. Calcd for $C_{160}H_{172}N_8{}^{58}Ni_2P_2{}^{194}Pt$: 2577.1509 $[M]^+$; UV/Vis (CH_2Cl_2): λ_{max} (ε [$M^{-1}cm^{-1}$]) = 446 (2.48×10^5), 551 (3.55×10^4), and 591 (1.67×10^4) nm.

Reductive elimination of 5 assisted by P*t*Bu$_3$: A flask containing **5** (10.8 mg, 5.0 μmol), HP*t*Bu$_3$·BF_4 (14.5 mg, 50 μmol), and K_2CO_3 (6.9 mg, 50 μmol) was purged with nitrogen and then charged with toluene (1.0 mL). The mixture was stirred at 120 °C for 3 h. The residue was diluted with CH_2Cl_2, and passed through a small plug of silica-gel with copious washings (CH_2Cl_2). After removal of the solvent *in vacuo*, the residue was separated by silica gel chromatography eluting with CH_2Cl_2/*n*-hexane (1:9). Recrystallization of the separated solids from CH_2Cl_2/MeOH gave **9** (4.9 mg, 2.6 μmol, 53%).

Chemical oxidation of 5 with Magic Blue: To a mixture of **5** (5.9 mg, 2.7 μmol) and CH_2Cl_2 (2.0 mL), Magic Blue (2.6 mg, 3.2 μmol) was added. The mixture was stirred at room temperature for 20 min. The residue was diluted with CH_2Cl_2/*n*-hexane, and passed through a small plug of silica-gel with copious washings (CH_2Cl_2/*n*-hexane). After removal of the solvent *in vacuo*, the residue was separated by silica gel chromatography eluting with CH_2Cl_2/*n*-hexane (1:10). Recrystallization of the separated solids from CH_2Cl_2/MeOH gave **9** (3.4 mg, 1.8 μmol, 67%).

Chemical oxidation of 6 with Magic Blue: To a mixture of **6** (6.6 mg, 2.7 μmol) and CH_2Cl_2 (2.0 mL), Magic Blue (2.6 mg, 3.2 μmol) was added. The mixture was stirred at room temperature for 20 min. The residue was diluted with CH_2Cl_2/*n*-hexane, and passed through a small plug of silica-gel with copious washings (CH_2Cl_2/*n*-hexane). After removal of the solvent *in vacuo*, the residue was separated by silica gel chromatography eluting with CH_2Cl_2/*n*-hexane (1:10). Recrystallization of the separated solids from CH_2Cl_2/MeOH gave **9** (3.8 mg, 2.0 μmol, 76%).

Electrochemical oxidation of 5: In the anodic chamber of an H-type divided cell were placed **5** (6.0 mg, 2.8 μmol) and 0.1 M *n*Bu_4NPF_6/CH_2Cl_2 (8 mL). In the cathodic chamber was placed 0.1 M *n*Bu_4NPF_6/CH_2Cl_2 (7 mL). The constant current electrolysis (100 μA) was carried out at room temperature with magnetic stirring for 45 min. The solution in the anodic chamber was collected. The crude mixture was washed with a saturated aqueous $NaHCO_3$ solution and brine, and dried over anhydrous Na_2SO_4. After removal of the solvent *in vacuo*, the residue was separated by silica gel chromatography eluting with CH_2Cl_2/*n*-hexane (1:10). Recrystallization of the separated

solids from CH_2Cl_2/MeOH gave **9** (3.7 mg, 2.0 μmol, 72%).

Electrochemical oxidation of 6: In the anodic chamber of an H-type divided cell were placed **6** (6.7 mg, 2.7 μmol) and 0.1 M *n*Bu_4NPF_6/CH_2Cl_2 (8 mL). In the cathodic chamber was placed 0.1 M *n*Bu_4NPF_6/CH_2Cl_2 (7 mL). The constant current electrolysis (100 μA) was carried out at room temperature with magnetic stirring for 44 min. The solution in the anodic chamber was collected. The crude mixture was washed with a saturated aqueous $NaHCO_3$ solution and brine, and dried over anhydrous Na_2SO_4. After removal of the solvent *in vacuo*, the residue was separated by silica gel chromatography eluting with CH_2Cl_2/*n*-hexane (1:10). Recrystallization of the separated solids from CH_2Cl_2/MeOH gave **9** (3.9 mg, 2.1 μmol, 77%).

3. NMR Spectra

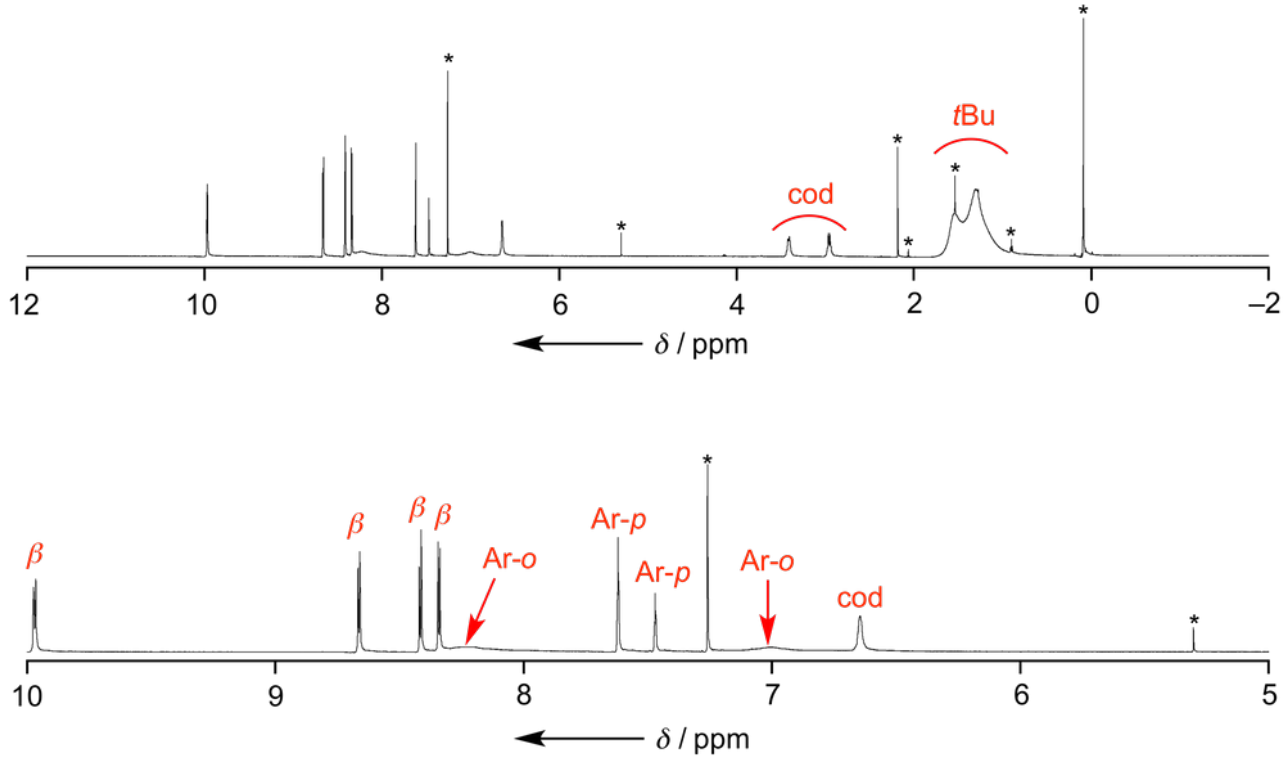

Figure S 1. The ^{1}H NMR spectrum of **5** in $CDCl_3$ at 25 °C. *Solvent and impurities.

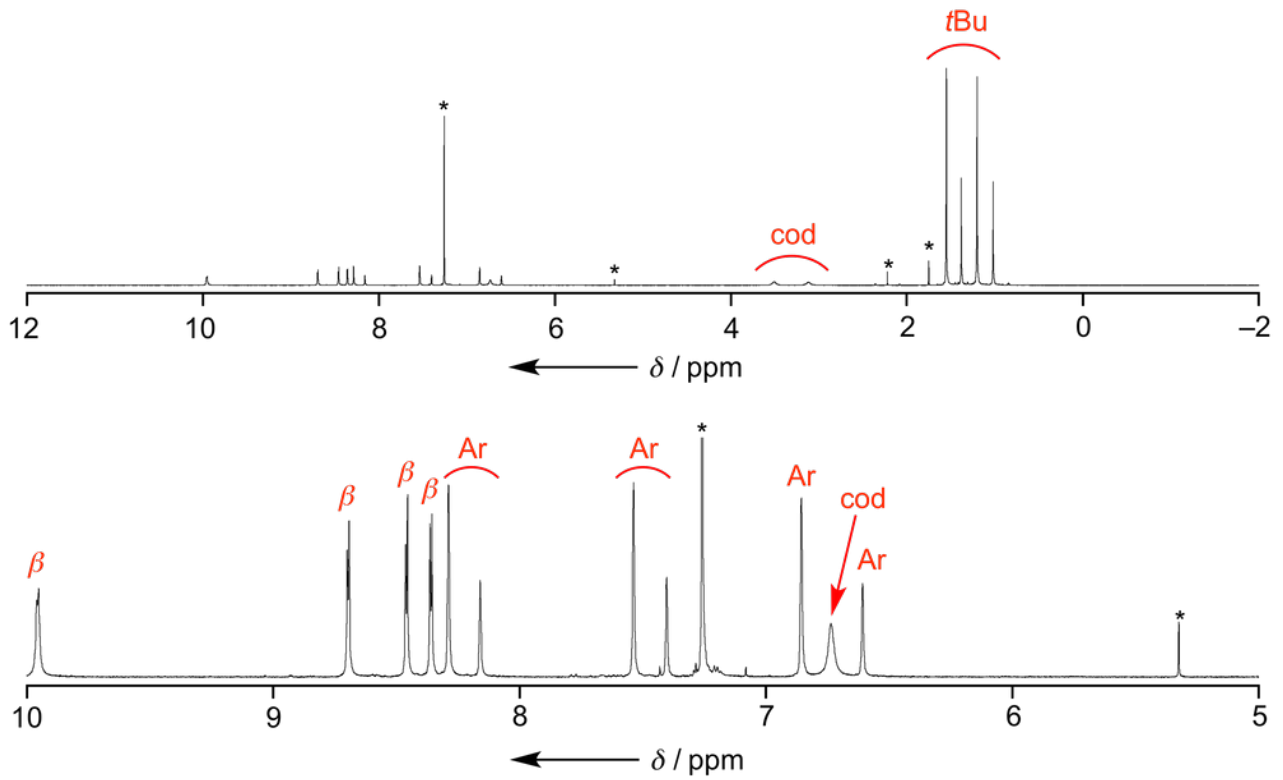

Figure S 2. The ^{1}H NMR spectrum of **5** in $CDCl_3$ at –60 °C. *Solvent and impurities.

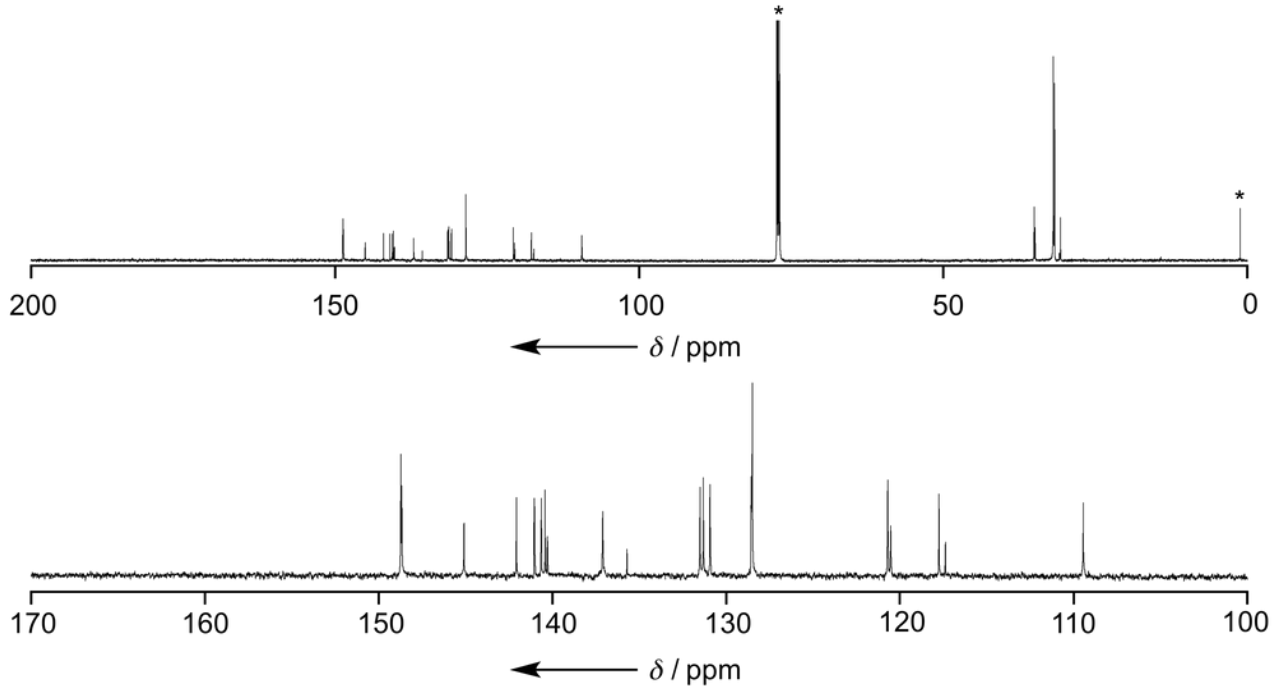

Figure S 3. The ^{13}C NMR spectrum of **5** in $CDCl_3$ at 50 °C. *Solvent and impurities.

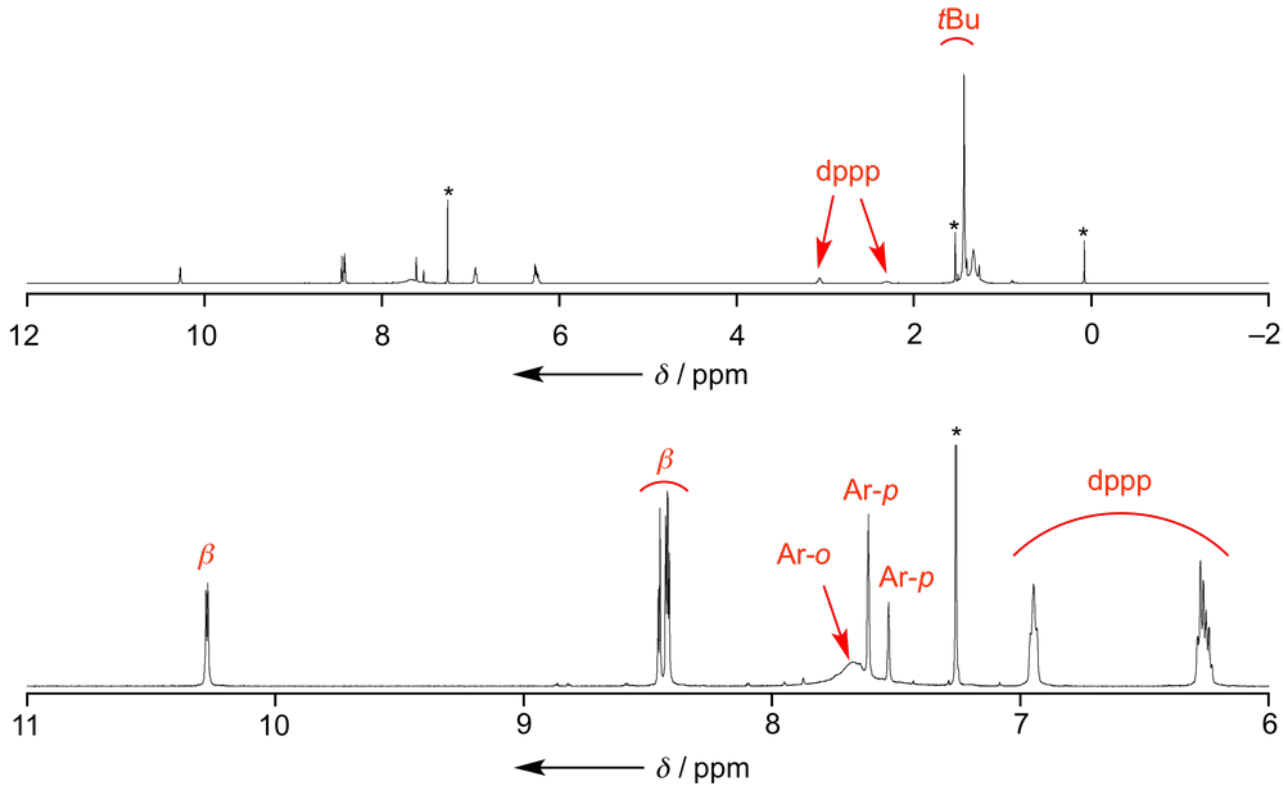

Figure S 4. The ^{1}H NMR spectrum of **6** in $CDCl_3$ at 25 °C. *Solvent and impurities.

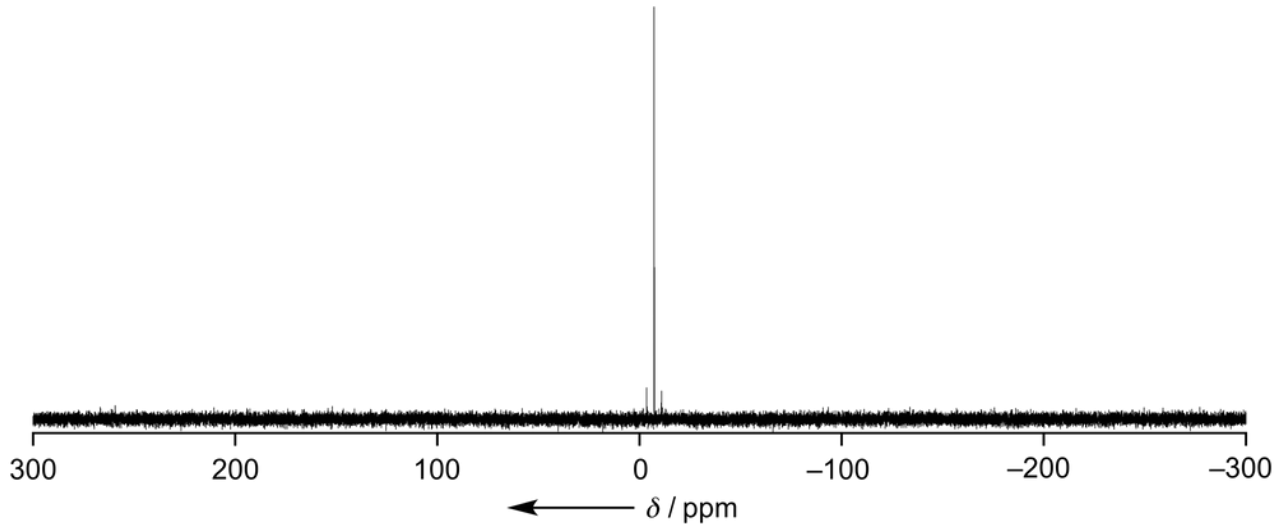

Figure S 5. The ^{31}P NMR spectrum of **6** in $CDCl_3$ at 25 °C.

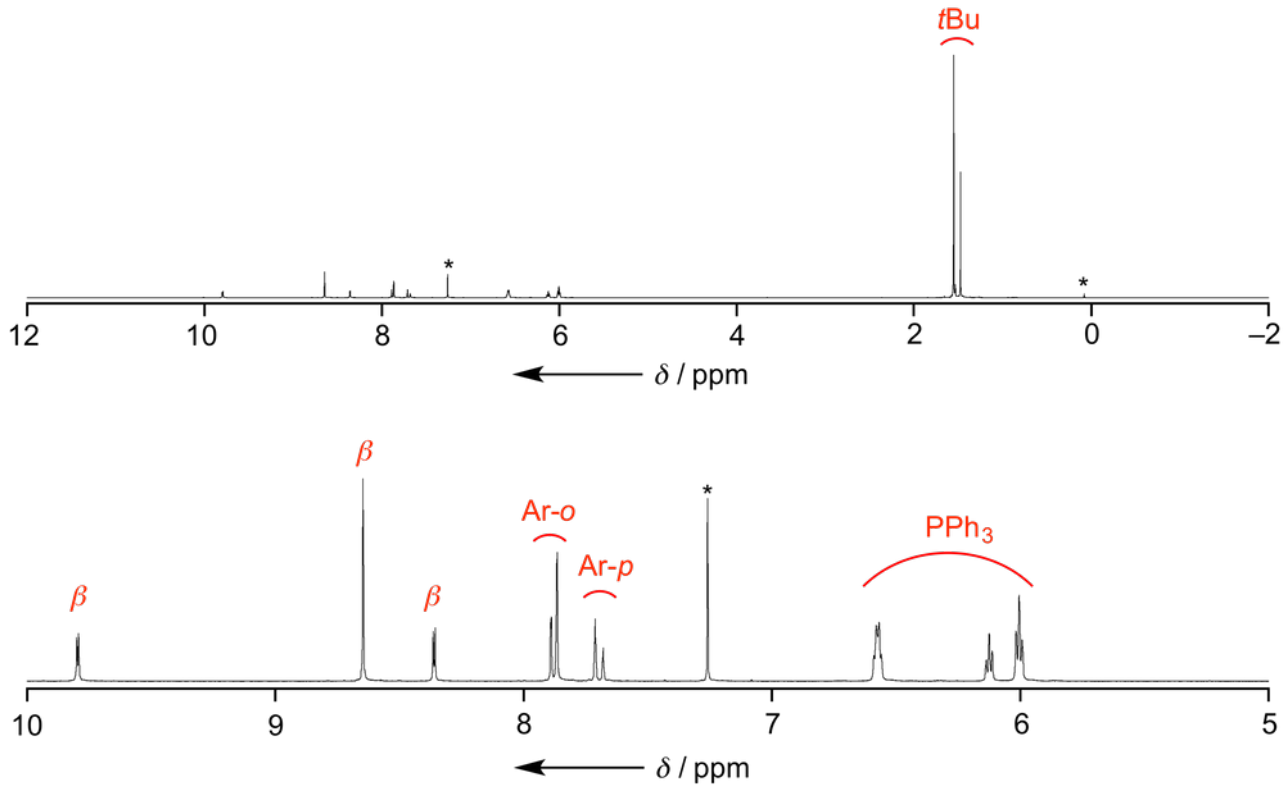

Figure S 6. The ^{1}H NMR spectrum of **7** in $CDCl_3$ at 25 °C. *Solvent and impurities.

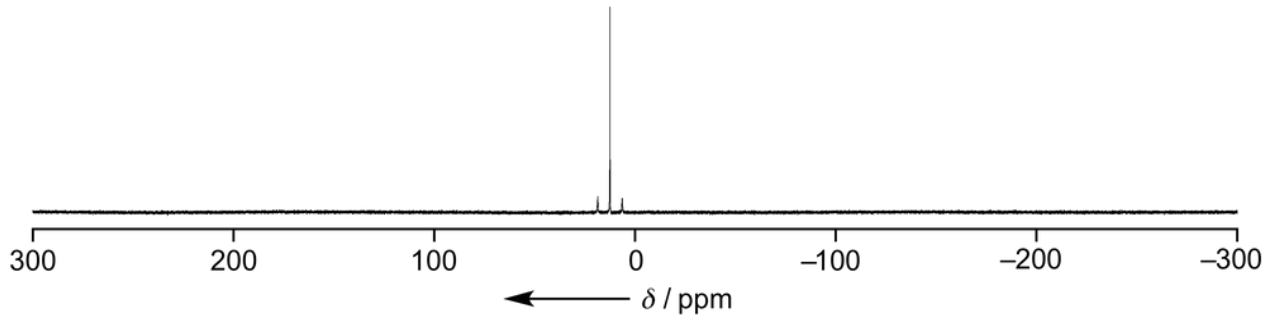

Figure S 7. The ^{31}P NMR spectrum of **7** in $CDCl_3$ at 25 °C.

4. Mass Spectra

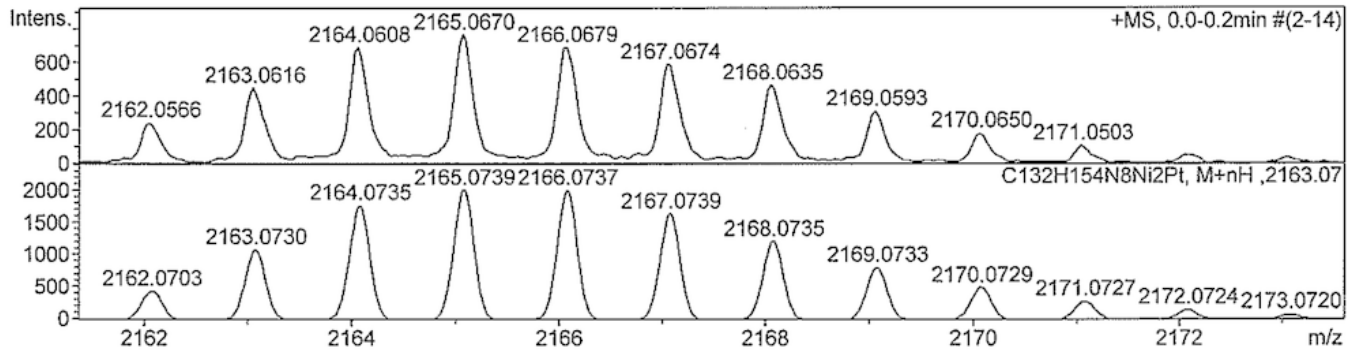

Figure S 8. Observed (top) and simulated (bottom) HR-ESI-TOF MS spectra of **5**.

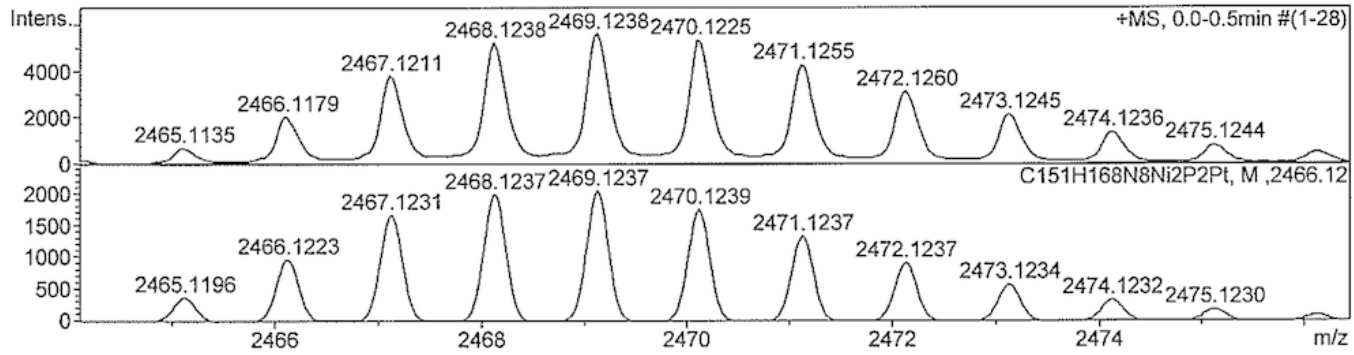

Figure S 9. Observed (top) and simulated (bottom) HR-ESI-TOF MS spectra of **6**.

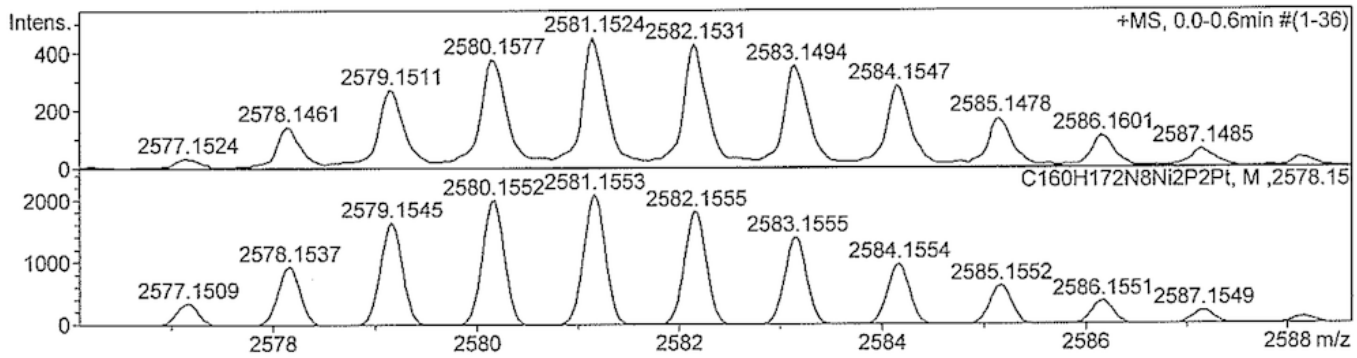

Figure S 10. Observed (top) and simulated (bottom) HR-ESI-TOF MS spectra of **7**.

5. X-Ray Crystal Structures

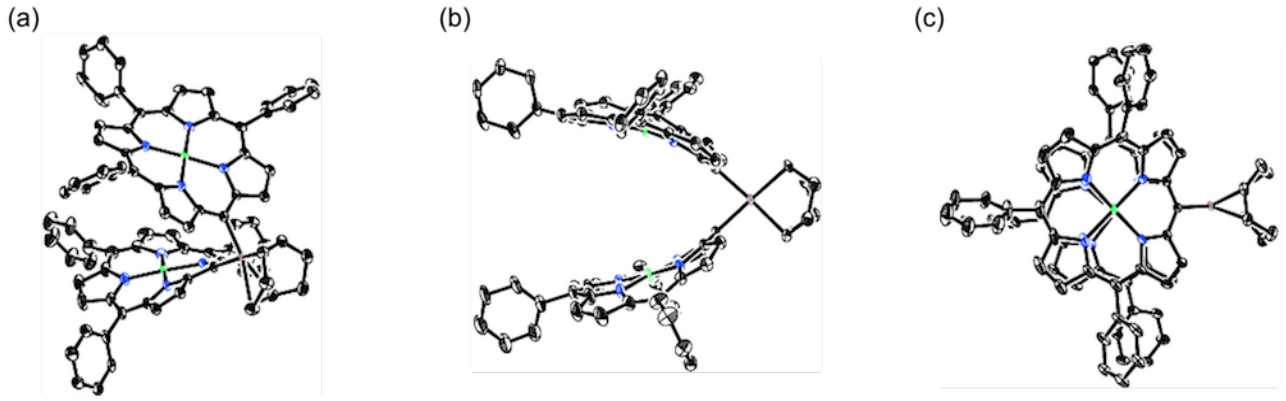

Figure S 11. The X-ray crystal structure of **5**. (a) Diagonal view, (b) side view, and (c) top view. Thermal ellipsoids are shown at the 50% probability level. Solvent molecules, *tert*-butyl groups, and all hydrogen atoms are omitted for clarity.

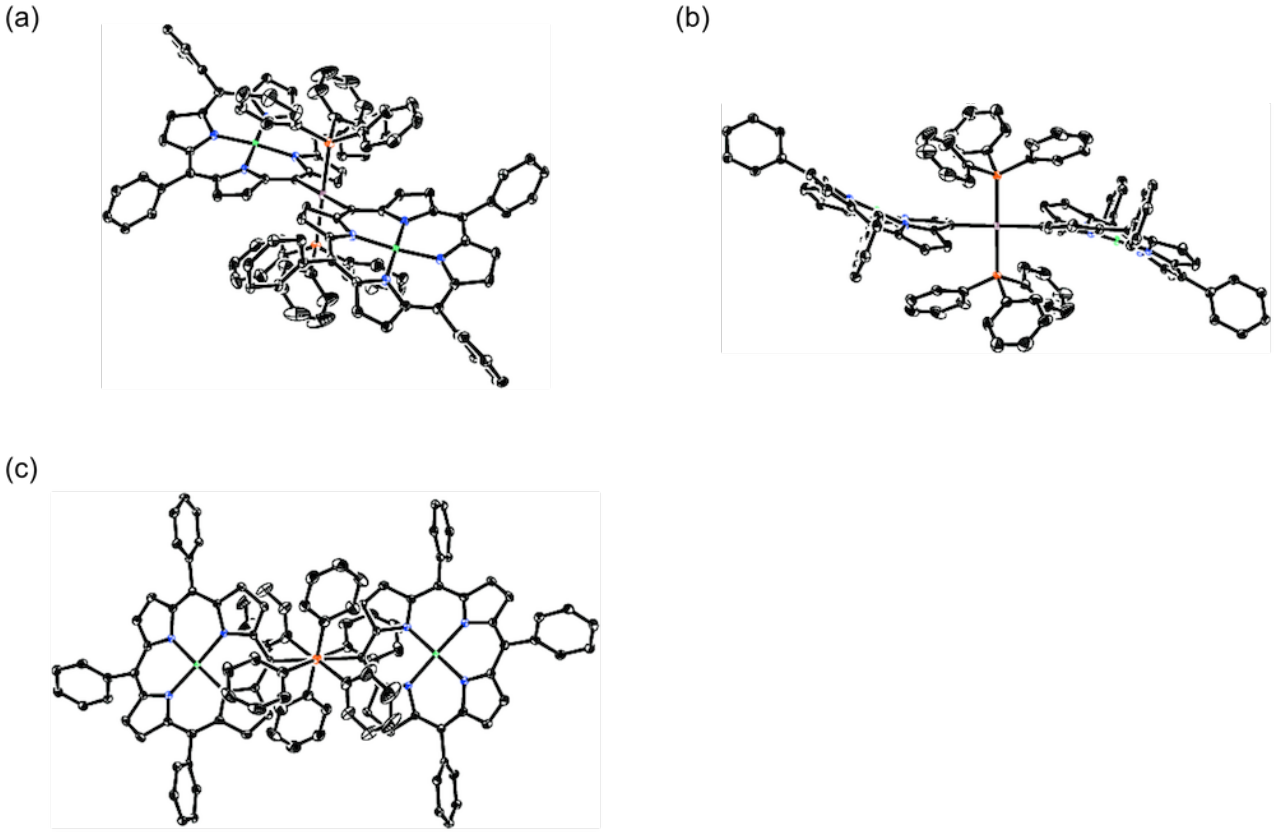

Figure S 12. The X-ray crystal structure of **7**. (a) Diagonal view, (b) side view, and (c) top view. Thermal ellipsoids are shown at the 50% probability level. Solvent molecules, *tert*-butyl groups, and all hydrogen atoms are omitted for clarity.

Table S 1. Crystal data and structure refinements for **5** and **7**.

Compound	**5**	**7**
Empirical Formula	$C_{132}H_{154}N_8Ni_2Pt$, $5(C_6H_4Cl_2)$	$C_{160}H_{172}N_8Ni_2P_2Pt$, $6(C_6H_5CH_3)$
Mw	2900.09	3134.27
Crystal System	Triclinic	Triclinic
Space Group	*P*-1 (No.2)	*P*-1 (No.2)
a	16.142(3) Å	15.566(2) Å
b	21.227(4) Å	15.8310(16) Å
c	22.446(4) Å	17.7553(19) Å
α	106.100(5)°	80.813(6)°
β	92.132(1)°	89.907(11)°
γ	93.364(6)°	88.251(9)°
Volume	7365(2) $Å^3$	4317.2(8) $Å^3$
Z	2	1
Density (calcd.)	1.308 g/cm^3	1.206 g/cm^3
Completeness	0.955	0.960
Goodness-of-fit	1.054	1.042
R_1 [$I>2\sigma(I)$]	0.0581	0.0313
wR_2 (all data)	0.1669	0.0810
Solvent System	$C_6H_4Cl_2$/MeCN	toluene/EtOH
CCDC No.	1529198	1529199

6. Electrochemical Properties

Cyclic voltammograms and differential pulse voltammograms were obtained under the following conditions; solvent: CH_2Cl_2, electrolyte: 0.1 M nBu$_4$NPF$_6$, working electrode: glassy carbon, counter electrode: Pt, reference electrode: Ag/AgClO$_4$, scan rate: 0.05 V/s.

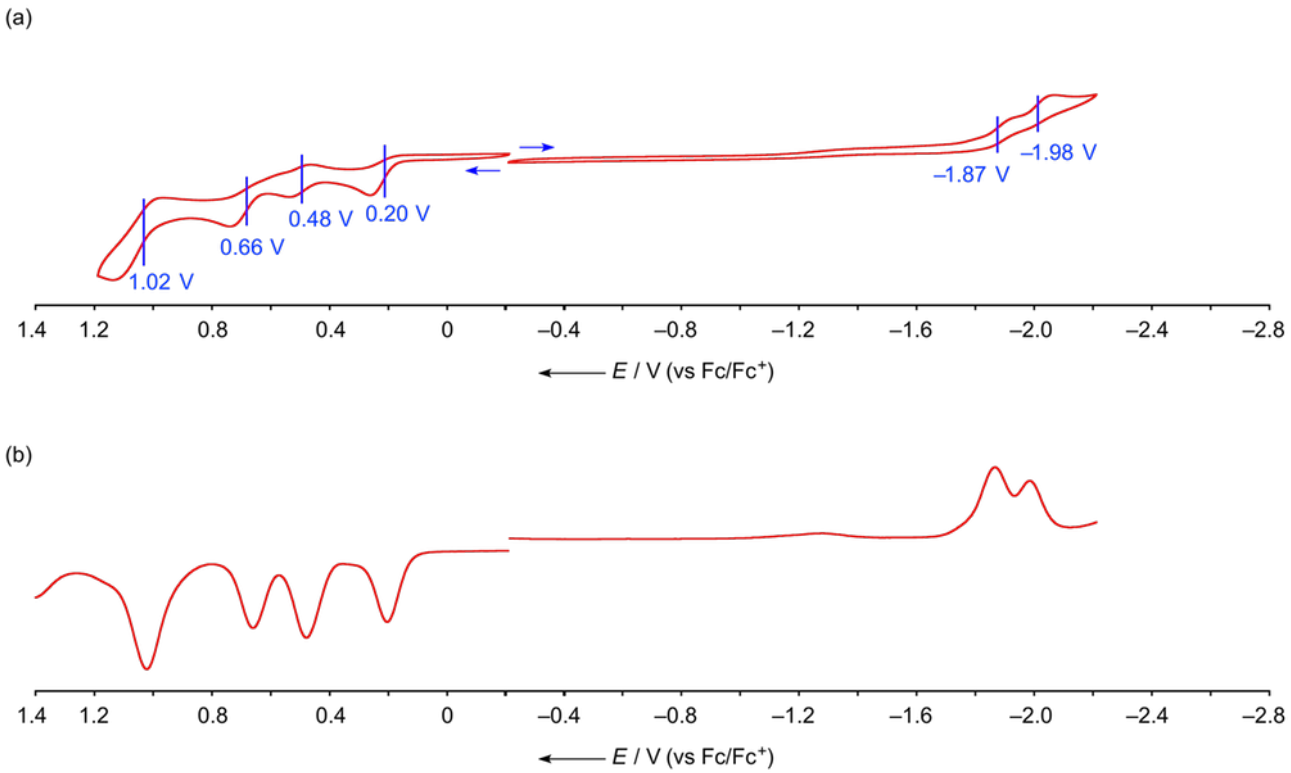

Figure S 13. (a) Cyclic voltammograms and (b) differential pulse voltammograms of **5**.

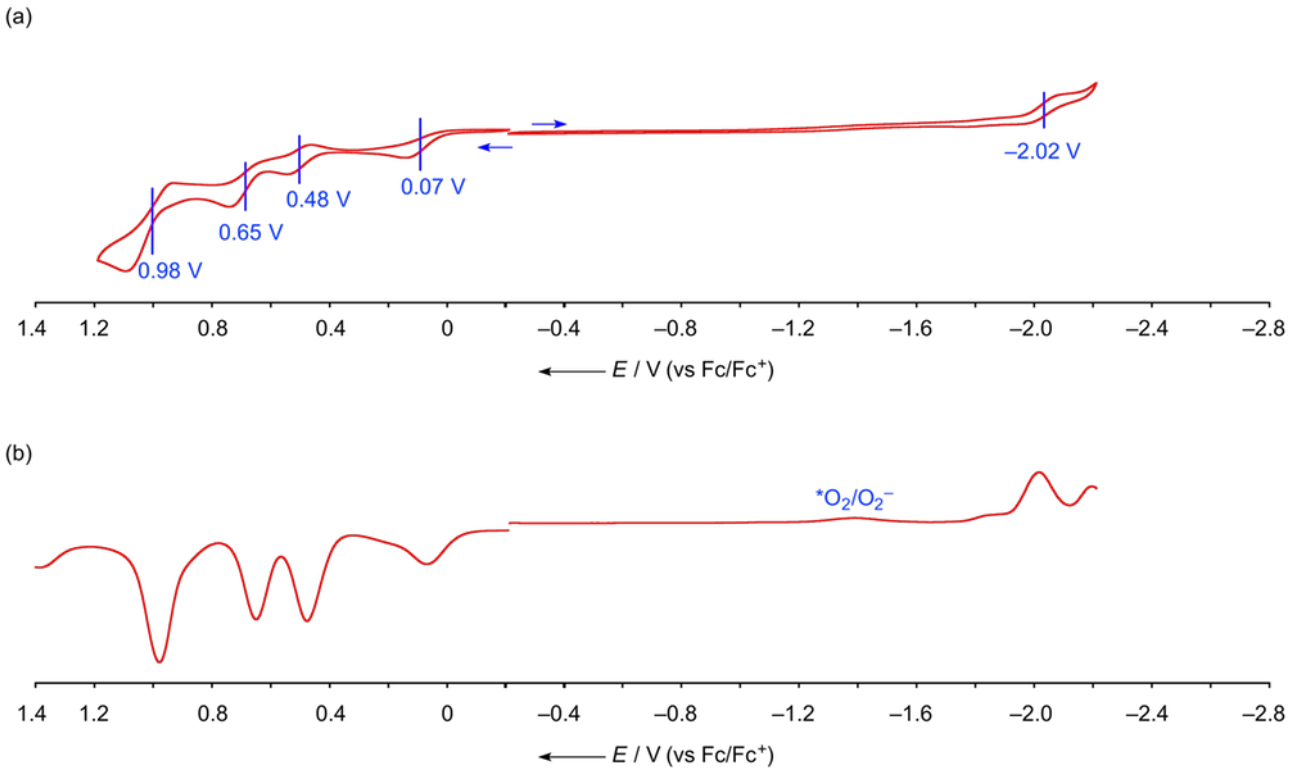

Figure S 14. (a) Cyclic voltammograms and (b) differential pulse voltammograms of **6**.

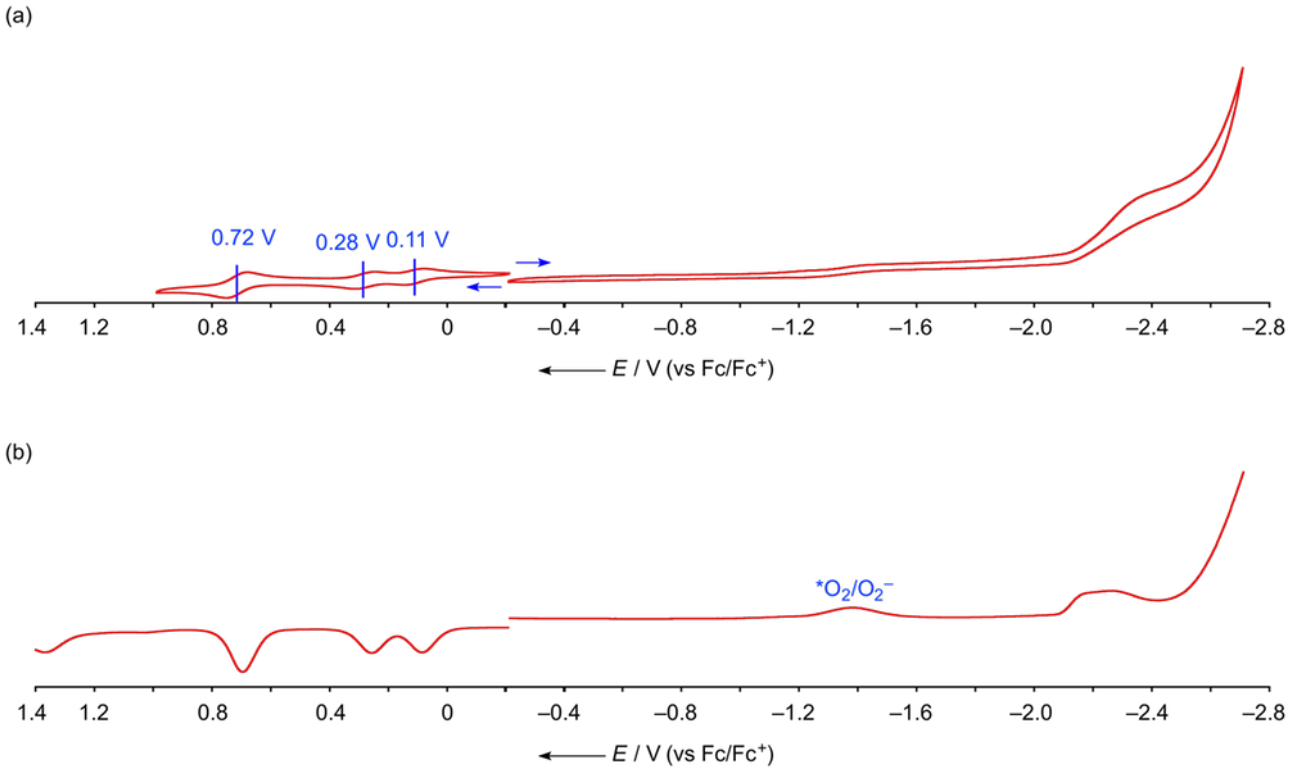

Figure S 15. (a) Cyclic voltammograms and (b) differential pulse voltammograms of **7**.

7. DFT Calculations

All calculations were carried out using *Gaussian 09* program.[S5] Initial geometries of **13_cis** and **13_trans** were based on the X-ray crystal structures of **5** and **7**, respectively. All structures were fully optimized without any symmetry restriction. The calculations were performed by density functional theory (DFT) method with restricted B3LYP (Becke's three-parameter hybrid exchange functionals and Lee-Yang-Parr correlation functional)[S6] level, employing basis sets 6-31G(d) for C, H, N, and P and LANL2DZ for Ni and Pt. *tert*-Butyl groups of **12** were replaced with hydrogen atoms to simplify the calculation.

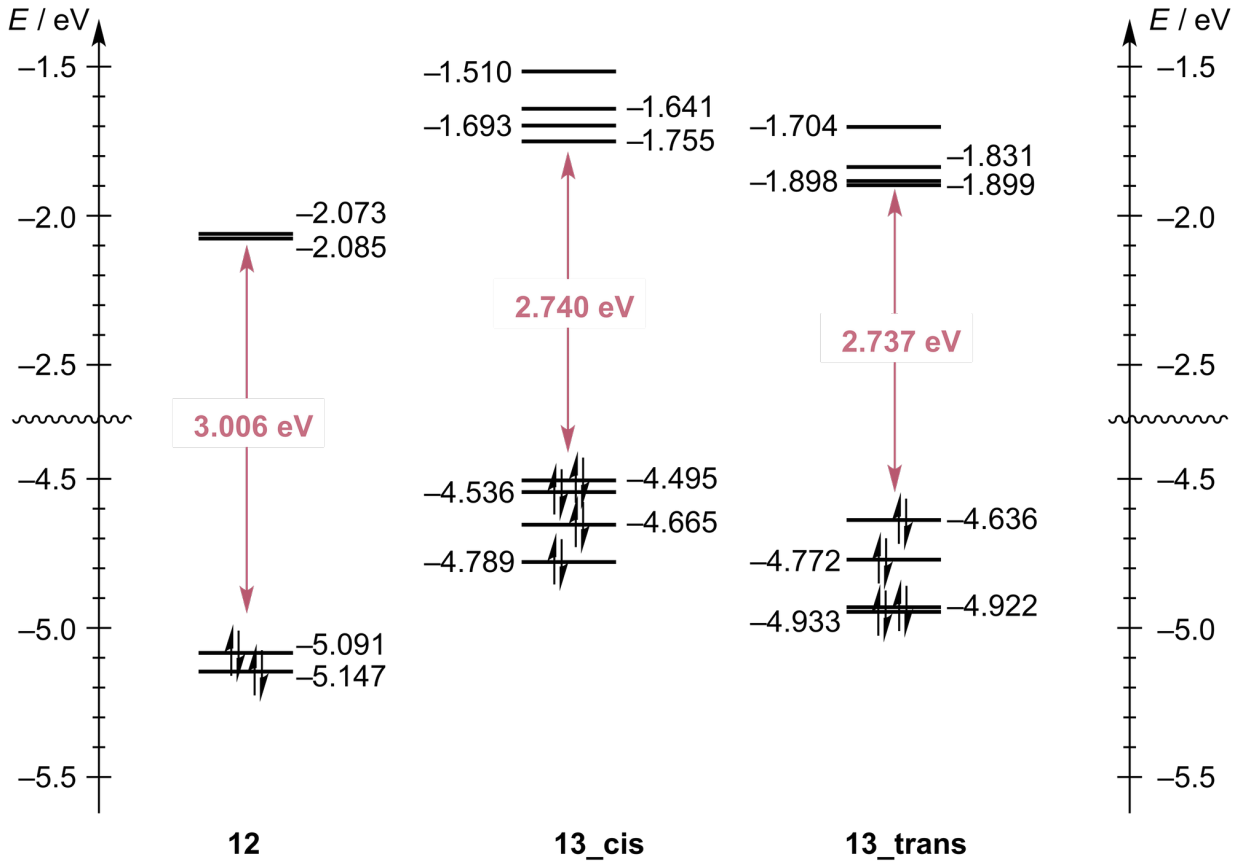

Figure S 16. Energy diagrams of **12**, **13_cis**, and **13_trans**.

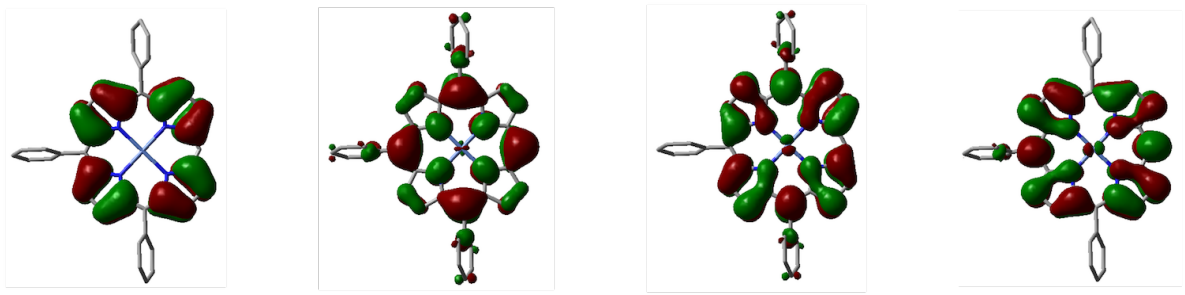

Figure S 17. Kohn-Sham orbital representations of **12** (isovalue = 0.02).

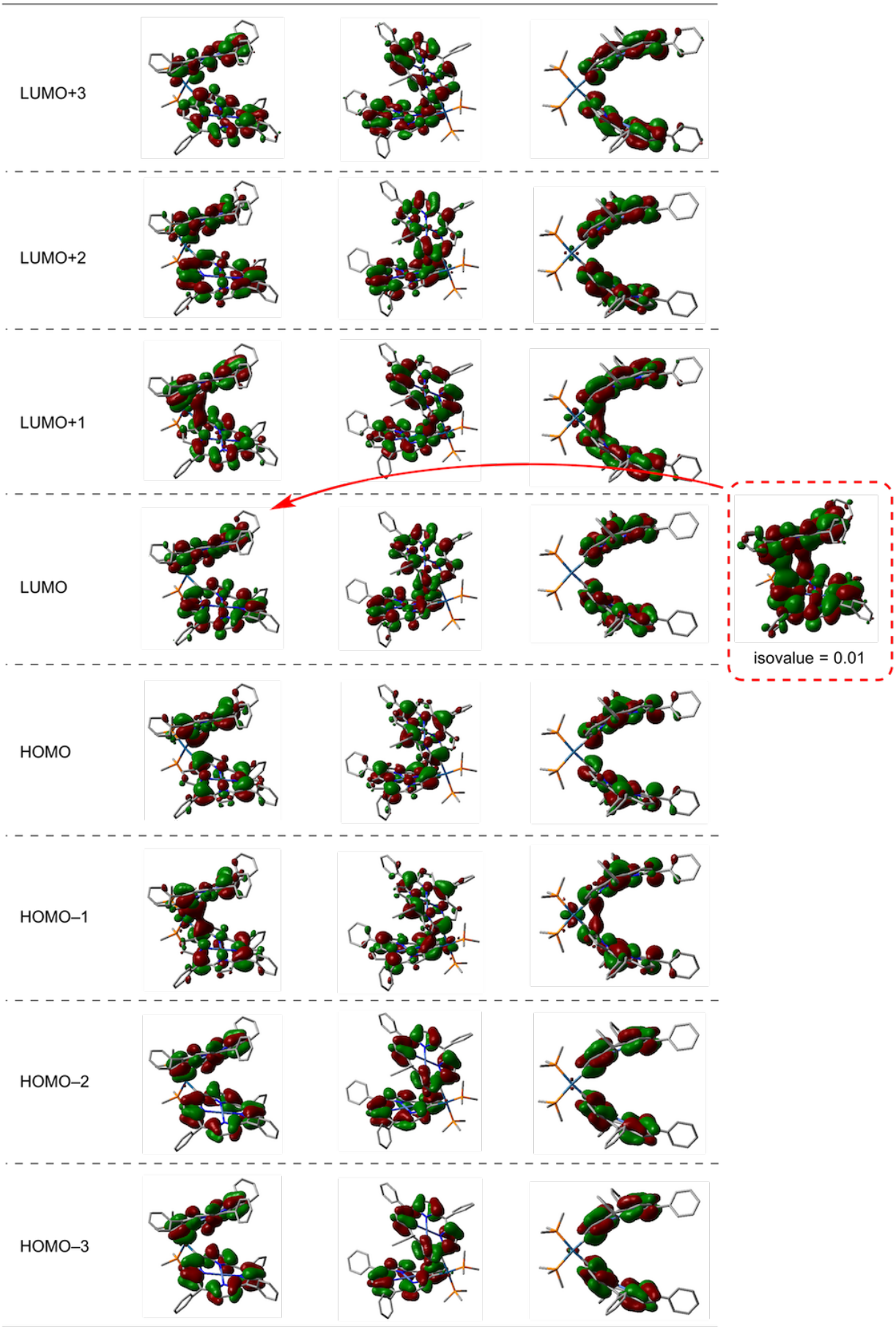

Figure S 18. Kohn-Sham orbital representations of **13_cis** (isovalue = 0.02).

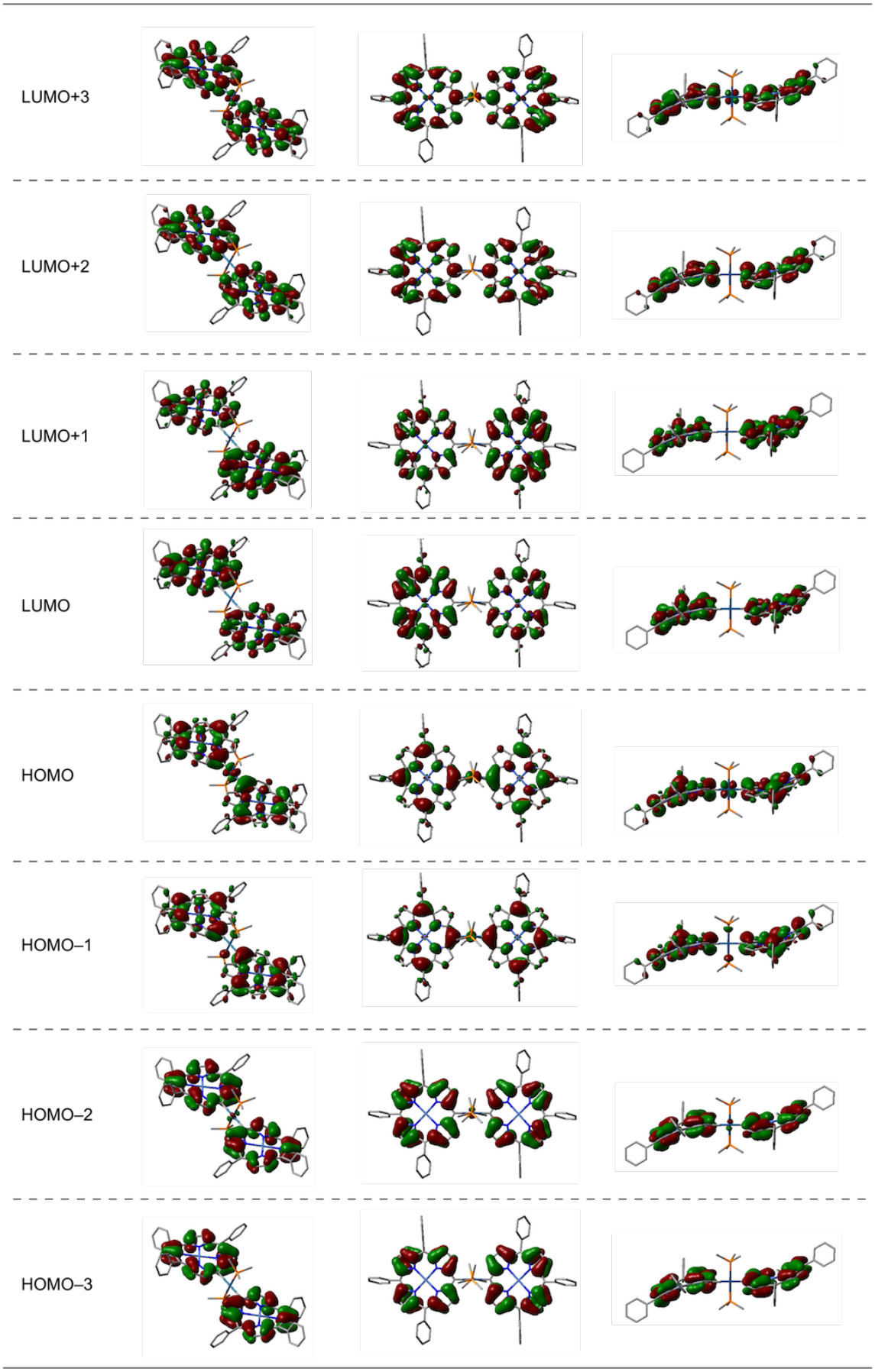

Figure S 19. Kohn-Sham orbital representations of **13_trans** (isovalue = 0.02).

8. References

[S1] A. Altomare, M. C.Burla, M. Camalli, G. Cascarano, C. Giacovazzo, A. Guagliardi, A. G. G. Moliterni, G. Polidori and R. Spagna, *J. Appl. Cryst.*, 1999, **32**, 115.

[S2] G. M. Sheldrick, *Acta Cryst*., 2008, **A64**, 112.

[S3] G. M. Sheldrick, *Acta Cryst*., 2015, **A71**, 3.

[S4] (a) G. M. Sheldrick, T. R. Schneider, *Methods Enzymol.*, 1997, **277**, 319. (b) G. M. Sheldrick, *Acta Cryst*., 2015, **C71**, 3.

[S5] Gaussian 09, Revision E.01, M. J. Frisch, G. W. Trucks, H. B. Schlegel, G. E. Scuseria, M. A. Robb, J. R. Cheeseman, G. Scalmani, V. Barone, B. Mennucci, G. A. Petersson, H. Nakatsuji, M. Caricato, X. Li, H. P. Hratchian, A. F. Izmaylov, J. Bloino, G. Zheng, J. L. Sonnenberg, M. Hada, M. Ehara, K. Toyota, R. Fukuda, J. Hasegawa, M. Ishida, T. Nakajima, Y. Honda, O. Kitao, H. Nakai, T. Vreven, J. A. Montgomery, Jr., J. E. Peralta, F. Ogliaro, M. Bearpark, J. J. Heyd, E. Brothers, K. N. Kudin, V. N. Staroverov, R. Kobayashi, J. Normand, K. Raghavachari, A. Rendell, J. C. Burant, S. S. Iyengar, J. Tomasi, M. Cossi, N. Rega, J. M. Millam, M. Klene, J. E. Knox, J. B. Cross, V. Bakken, C. Adamo, J. Jaramillo, R. Gomperts, R. E. Stratmann, O. Yazyev, A. J. Austin, R. Cammi, C. Pomelli, J. W. Ochterski, R. L. Martin, K. Morokuma, V. G. Zakrzewski, G. A. Voth, P. Salvador, J. J. Dannenberg, S. Dapprich, A. D. Daniels, O. Farkas, J. B. Foresman, J. V. Ortiz, J. Cioslowski and D. J. Fox, Gaussian, Inc.: Wallingford, CT, 2009.

[S6] a) A. D. Becke, *J. Chem. Phys.*, 1993, **98**, 1372; b) C. Lee, W. Yang and R. G. Parr, *Phys. Rev. B*, 1998, **37**, 785.